Journal of Dentistry 166 (2026) 106513

Contents lists available at ScienceDirect

Journal of Dentistry

journal homepage: www.elsevier.com/locate/jdent

Does localized irradiance of poly-wave LED influence the bonding performance of universal adhesives to dentin?

E Sutil [a], M Wendlinger [b,c], AFM Cardenas [d], FSF de Siqueira [e], CJ Soares [f], S Geraldeli [g], AD Loguercio [b,*]

[a] Department of Restorative Dentistry, Ponta Grossa State University, Ponta Grossa, Paraná, Brazil
[b] Department of Restorative Dentistry, Ponta Grossa State University, Rua Carlos Cavalcanti, 4748, Bloco M, Sala 64A – Uvaranas, Ponta Grossa, Paraná 84030-900, Brazil
[c] Department of Restorative Dentistry and Cariology, Adhesive Dentistry Research Group, Institute of Dentistry, University of Turku, Turku, Finland
[d] Department of Restorative Dentistry, School of Dentistry, Federal University of Maranhão, UFMA, São Luís, Brazil
[e] Department of Restorative Dentistry, Ceuma University, São Luís, Maranhão, Brazil
[f] Department of Operative Dentistry and Dental Materials, School of Dentistry, Federal University of Uberlandia, Uberlandia, Minas Gerais, Brazil
[g] Department of General Dentistry, School of Dental Medicine, East Carolina University, Greenville, NC, USA

ARTICLE INFO

Keywords:
Polymerization
Dental adhesives
Camphoroquinone
Light-curing units

ABSTRACT

Purpose: This study evaluates how different wavelength ranges emitted by a poly-wave LED curing light violet (405 nm) and blue (445 and 465 nm) affect the microtensile bond strength (μTBS), nanoleakage (NL), and in situ degree of conversion (DC) of universal adhesives applied to dentin.
Methods: Eighty caries-free human molars were randomly assigned to four groups according to two variables: (1) Adhesive system (Ambar Universal APS [AMU], Scotchbond Universal [SBU] and (2) application mode (etch-and-rinse [ER] or self-etch [SE]). To control tooth dependency, each tooth quadrant of every tooth was allocated to a different wavelength range (405, 445 and 465 nm) and identified accordingly during light-curing with the Valo unit (1400 mW/cm^2). Afterwards, resin composite fillings were placed, and each quadrant was sectioned to obtain resin-dentin bonded beams (0.8 mm^2). These beams were tested for μTBS, NL, and DC. Data for μTBS (MPa), NL (%), and DC (%) were analyzed using three-way ANOVA and Tukey's test (α=5%).
Results: For AMU and SBU, no significant differences were observed among the 445-nm and 465-nm wavelength ranges ($p > 0.05$) for all outcomes. However, light curing SBU with 405-nm LED resulted in significantly lower μTBS and DC values and higher NL values compared with 445 and 465 nm LEDs ($p < 0.01$). AMU exhibited higher μTBS and DC values than SBU ($p = 0.001$). No significant differences were found between SE and ER application strategies ($p > 0.05$).
Clinical significance: Bonding to dentin may be locally compromised when universal adhesives relying on the conventional camphorquinone/amine photoinitiator system are light-cured with poly-wave LEDs that exhibit non-uniform spectral distribution.

1. Introduction

Adhesive dentistry has undergone remarkable progress over the past decades, largely driven by the development of resin-based materials and improved light-curing technologies [1]. The effectiveness and long-term durability of adhesive procedures fundamentally rely on both the adhesive's chemical formulation and achieving a correct polymerization process [2,3]. To ensure proper curing, photoinitiators (PIs) within the adhesive play a critical role by initiating polymerization upon exposure to specific light wavelengths [4]. For decades, the most common PI system used in dental adhesives and composites has been camphorquinone (CQ) combined with a tertiary amine as co-initiator [5]. Even though the tertiary amine co-initiator boosts polymerization [6], this system faces two major challenges in modern simplified adhesives. First, the low pH characteristic of many simplified adhesives may neutralize the tertiary amine through acid-based reactions, thereby reducing its

* Corresponding author.
E-mail addresses: sutillisa@yahoo.com.br (E. Sutil), mwecan@utu.fi (M. Wendlinger), andresfelipemillancardenas@hotmail.com (A. Cardenas), fabisfsiqueira@hotmail.com (F. de Siqueira), carlosjsoares@ufu.br (C. Soares), geraldelis19@ecu.edu (S. Geraldeli), alelog@uepg.br (A. Loguercio).

https://doi.org/10.1016/j.jdent.2026.106513
Received 9 December 2025; Received in revised form 13 January 2026; Accepted 15 January 2026
Available online 16 January 2026

efficacy [7]. Second, simplified adhesives contain water (necessary to ionize acidic monomers), and their inherently hydrophilic nature attracts additional water osmotically from the underlying dentin [8]. This significantly presence of water may further reduce the efficiency of the relatively hydrophobic CQ, ultimately compromising the overall bonding performance.

To overcome this limitation, alternative PIs such as Lucirin TPO (mono-acylphosphine oxide), PPD (1-phenyl-1,2-propanedione), DMBZ (2,2-dimethoxy-1,2-diphenylethanone), and mixed thereof have been incorporated into newer resin-based formulations [3,9–11]. These PIs are Norrish type I PIs (molecules that undergo cleavage upon ultraviolet light excitation to generate free radicals). Due to their lower molecular weight, the absence of amine and higher reactivity, they exhibit greater water compatibility and lower yellowing compared to CQ [9,12,13]. However, CQ primarily absorbs in the blue region (450–470 nm) [14], while these alternative PIs absorb in the ultraviolet–violet region (< 420 nm) [15]. This spectral mismatch renders them incompatible with single-peak LED light-curing units (LCUs) (first- and second-generation), which emit only blue light (420–490 nm) [3,16].

Consequently, manufactures developed new-generation LCUs with broader emission spectra encompassing both blue and violet wavelengths [4,16,17]. These "multispectrum' or "poly-wave" devices combine multiple LED chips with different emission peaks to generate a wider light spectrum, thus increasing their potential to effectively cure dental materials containing various PIs [17]. However, because LED chips are positioned individual at a specific location within the array, the emitted light may present an uneven wavelength distribution [18]. As a result, some regions of the material may predominantly receive blue light, while others are exposed mainly to violet light [18–20]. This heterogeneous distribution is a significant concern. For example, Price et al. (2010) [18] demonstrated that this nonuniform emission is closely related to the spatial arrangement of LED chips within the LCUs head. This uneven light distribution can have clinical implications, as it may negatively affect the mechanical properties of resin composites [21–23]. Because adhesives systems share compositional similarities with resin composites, this issue may also pose challenges for the proper photoactivation of adhesives that incorporate alternative PIs.

While some studies have evaluated this correlation and reported no detrimental effects when poly-wave LCUs were used with adhesive systems containing alternative PIs [6], most of these investigations focused on root dentin [24,25] or on the effects of irradiance and exposure time [26]. Crucially, they failed to characterize the LCUs or distinguishing between areas corresponding to each wavelength (i.e., blue and violet). Given the distinct characteristics of root and coronal dentin (e.g., moisture content and permeability) and the known nonuniformity of LCUs wavelength distribution emitted by, evaluating these aspects in coronal dentin appears scientifically justified.

Therefore, this study aimed to evaluate the influence of localized wavelength ranges (violet 405 nm vs. blue 445 and 465 nm) emitted by a poly-wave LED LCU on the bonding performance of universal adhesives containing different PIs when applied to coronal dentin. Microtensile bond strength, nanoleakage, and in situ degree of conversion were assessed, considering both the adhesive formulation and the application mode (etch-and-rinse or self-etch). The null hypotheses tested were that the wavelength range would not affect *(i)* microtensile bond strength, *(ii)* nanoleakage, or *(iii)* in situ degree of conversion of universal adhesives to dentin regardless of application mode.

2. Material and methods

2.1. Experimental design

The present study evaluated three factors affecting adhesive performance: (1) adhesive system**,** with two levels (Scotchbond Universal [SBU] and Ambar Universal APS [AMU]**);** (2) adhesive strategy, with two levels (etch-and-rinse or self-etch); and **(**3) localized wavelength range**,** with three levels (LED spectral peaks centered at 405, 445, and 465 nm). Eighty sound human molars were randomly allocated to four primary experimental groups defined by the combination of adhesive system and adhesive strategy (n = 20 teeth/group). The wavelength factor was applied using a split-tooth design, in which each tooth received all three wavelength conditions in different quadrants, allowing each tooth to serve as its own control and minimizing tooth-related variability. (Fig. 1A, B).

2.2. Selection and preparation of teeth

Eighty caries-free human molars were used in this study. All teeth were collected after obtaining the patients' informed consent and with approval from the Research Ethics Committee of the State University of Ponta Grossa/PR/Brazil (protocol no. 3.542.383). Following extraction, we disinfected the teeth in 0.5 % chloramine, stored them in distilled water, and used them within six months.

Each tooth was sectioned parallel to the occlusal surface with a low-speed diamond saw (Isomet, Buehler, Lake Bluff, IL, USA) under water cooling to expose mid-coronal dentin. The surrounding enamel was removed using a diamond bur (#3195; KG Sorensen, Barueri, SP, Brazil). A standardized smear layer was created by grinding the flat dentin surfaces with #600-grit silicon carbide (SiC) paper under running water for 60 s.

2.3. Spectral evaluation

The light output of the VALO Cordless unit was measured using a MARC Patient Simulator (MARC-PS, BlueLight Analytics, Halifax, NS, Canada). Measurements were performed in standard mode for 10 s with the light tip positioned directly over the anterior MARC sensor at a distance of 0 mm. The sensor was connected to a laboratory-grade fiber optic spectrometer (USB4000, Ocean Optics, Dunedin, FL, USA) located inside the mannequin head. The MARC software was used to calculate absolute irradiance (mW/cm^2/nm) and generate the post-processed spectra output.

2.4. Restorative procedures

All teeth were fixed to a light-curing device to an x–y–z positioning system (Universal Light Curing Device Holder, Odeme, Luzerna, SC, Brazil) to ensure that each tooth quarter was exposed to light from each LED chip (Fig. 1A, B). This system, mounted on an optical bench, allowed us to achieve standardized alignment of the light beam precisely with the tooth surface (Fig. 1C, D). We color-coded the position of each LED (405 nm = violet; 445 nm = blue; 465 nm = red) and applied this identical color scheme to divide the occlusal surface of each tooth accordingly (Fig. 2A, B).

For the ER strategy, a 37 % phosphoric acid gel (Condac37, FGM Dental Group, Joinville, SC, Brazil) was applied to the dentin surfaces for 15 s, followed by rinsing with water for 30 s and gentle air-drying for 5 s. For the SE strategy, the dentin was left unconditioned. In both strategies, the adhesives were applied according to the manufacturer's instructions (Table 1), and light-cured for 1400 mW/cm^2 for 10 s (14 J/cm^2) (Fig. 1E).

Following the bonding procedures, composite build-ups (Opallis, FGM Dental Group, Joinville, SC, Brazil) were constructed in two to three increments of 2 mm. Each increment was light cured for 40 s at a distance of 1 mm using a LED LCU (Valo Cordless, Ultradent, South Jordan, UT, USA). All bonding procedures were performed by a single operator. Immediately afterward, the resin composite surface was color-marked using the previously described color scheme (Fig. 1F). This procedure ensures that each portion of the restored surface corresponded precisely to the LED wavelength used for its polymerization (violet, blue or red) (Fig. 1F, G).

The teeth were then stored in distilled water at 37 °C for 24 h. After

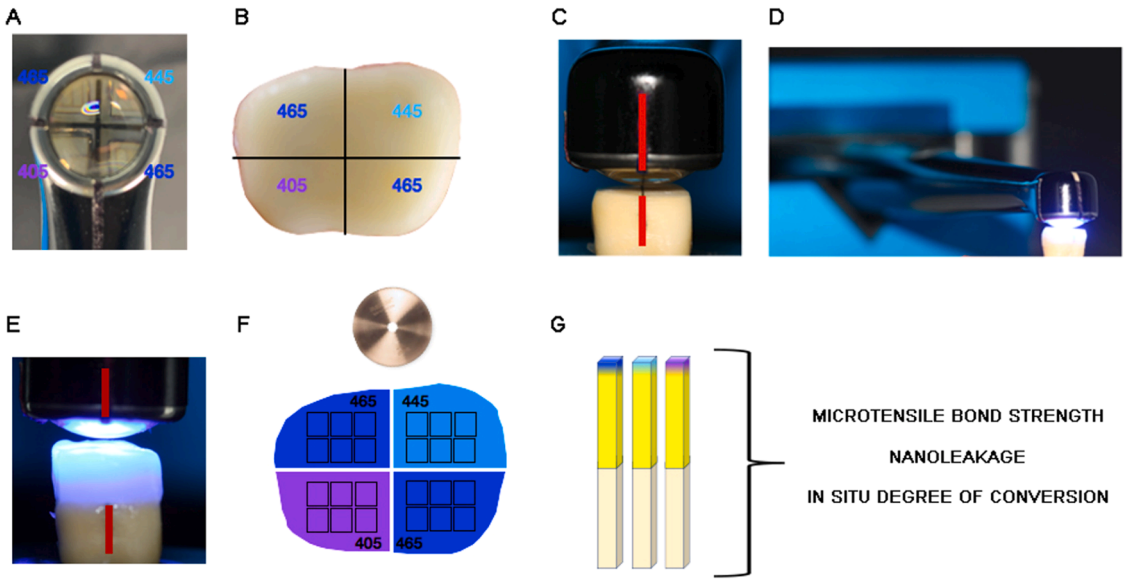

Fig. 1. Specimen Preparation Schematic. (A) The head of VALO Cordless light-curing unit was marked with an indicator line, according to the distribution of the different LEDs wavelength peaks, as well as (B) the corresponding wavelength ranges positioned on the dentin surfaces (C). To ensure precise positioning, both the VALO Cordless unit and the tooth were marked with an indicator line and placed in a x–y–z positioning system mounted on an optical bench (D). Valo tip aligned with the tooth mark and applied light to the lasty layer of the resin composite build-up (E), and color identification of each quadrant according to the different LEDs wavelength peaks (F). Small squares indicate how many possible beams could be obtained after sectioning with diamond blade. (G) Resin-dentin bonded sticks with one color-coded according to the LEDs wavelength peaks and the in vitro tests performed.

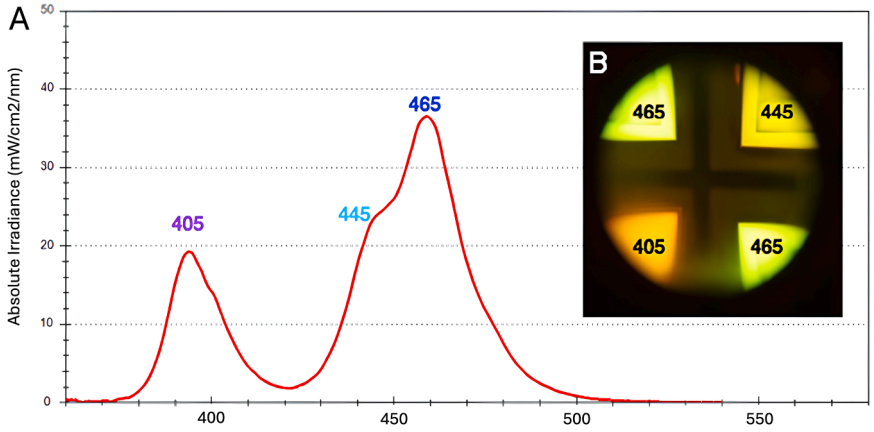

Fig. 2. (A) Schematic distribution of the LED wavelengths emitted by the VALO Cordless unit. (B). Absolute irradiance of the VALO Cordless in standard mode for 10 s on MARC system. Observe the distribution of the different LED wavelength peaks.

storage, they were sectioned in the mesiodistal and buccolingual directions using a precision cutting machine (Isomet, Buehler; Lake Bluff, IL, USA) to obtain resin-dentin bonded sticks with a cross-sectional area of approximately 0.8 mm^2, measured with digital calipers (Digimatic Caliper, Mitutoyo; Tokyo, Japan). The number of sticks exhibiting pre-test failure (PF) during specimen preparation was recorded for each tooth.

The resin–dentin bonded sticks obtained from each tooth and experimental condition were allocated as follows (Fig. 1G): two sticks were used for nanoleakage (NL) evaluation, and one stick was used to assess the in situ degree of conversion (DC) within the adhesive/hybrid layers. These analyses are interface-focused, high-resolution techniques that require a limited number of specimens. The remaining sticks (a minimum of eight per tooth) were used for microtensile bond strength (μTBS) testing, which requires a larger number of specimens to account for interfacial variability and to ensure adequate statistical reliability, in accordance with established methodological recommendations [27–29].

2.5. Microtensile bond strength testing

Microtensile bond strength testing followed the Academy of Dental Materials guidelines for non-trimmed μTBS testing [27]. A minimum of eight resin-dentin bonded sticks per tooth were randomly assigned and tested ($n = 20$ teeth/group). The sticks were attached to a Geraldeli's jig using cyanoacrylate adhesive and tested in tension (Kratos Dinamometros, Cotia, SP, Brazil) at a crosshead speed of 0.5 mm/min until failure. μTBS values (MPa) were calculated by dividing the maximum load at failure (N) by the cross-sectional bonding area (mm^2).

Failure modes were classified as cohesive ([C] failure exclusively within dentin or resin composite), adhesive/mixed ([A/M] failure at the resin-dentin interface, or interfacial failure combined with partial cohesive failure of adjacent substrates). Classification was performed under a stereomicroscope at 100 × magnification (Olympus SZ40, Tokyo, Japan). The number of premature failures (PF) was recorded and assigned a value of 0 MPa.

Table 1
Adhesive systems, batch number, composition and application modes.

Adhesive system (Batch number)	Composition	Application mode	
		Etch-and-rinse	Self-etch
Ambar Universal APS (AMB, FGM Dental Group, #080,622)	Methacrylate monomers (UDMA and 10-MDP), photoinitiators, coinitiators, stabilizers, inert silica nanoparticles and ethanol	1. Apply etchant for 15 s 2. Rinse thoroughly 3. Remove excess water with air 4. Apply adhesive as for the self-etch mode	1. Apply two coats vigorously by rubbing the adhesive for 20 s (10 s each) 2. Gently air dried for 10 s to evaporate the solvent 3. Light cured for 10 s at 1400 mW/cm^2
Scotchbond Universal (SBU, Solventum, #2417,600,159)	10-MDP, dimethacrylate resins, HEMA, methacrylatemodified polyalkenoic acid copolymer, nanofiller, ethanol, water, initiators, silane	1. Apply etchant for 15 s 2. Rinse thoroughly 3. Remove excess water with air 4. Apply adhesive as for the self-etch mode	1. Applied the adhesive to the entire preparation and left undisturbed for 20 s 2. Directed a gentle stream of air over the liquid for about 5 s until it no longer moved and the solvent was evaporated completely 3. Light cured for 10 s at 1400 mW/cm^2

Abbreviations: UDMA: urethane methacrylate; 10-MDP: 10-methacryloyloxydecyl dihydrogen phosphate; HEMA: 2-hydroxyethyl methacrylate.
* The materials were applied according to the recommendations of their respective manufacturers.

2.6. Nanoleakage evaluation

Two resin–dentin bonded sticks per group were randomly assigned for nanoleakage assessment. Each stick was coated with two layers of nail varnish, leaving a 1-mm window around the bonded interface exposed. Specimens were rehydrated in distilled water for 10 min before immersion in a silver nitrate tracer solution for 24 h. Ammoniacal silver nitrate was prepared according to Tay et al. [28]. Sticks were immersed in a 50 wt % ammoniacal silver nitrate solution in total darkness for 24 h, rinsed thoroughly, and then immersed in a photo-developing solution under fluorescent light for 8 h to reduce silver ions into metallic silver grains within nanoporosities of the bonded interface.

Specimens were sequentially wet-polished using 1000-, 1500-, 2000-, and 2500-grit SiC paper, followed by polishing with 1 μm and 0.25 μm diamond pastes (Buehler Ltd., Lake Bluff, IL, USA). The sticks were ultrasonically cleaned, air-dried overnight, and gold sputter-coated (MED 010, Balzers Union, Balzers, Liechtenstein). Bonded interfaces were examined under a scanning electron microscope (SEM) in backscattered electron mode at 15 kV (VEGA 3, TESCAN, Shimadzu, Tokyo, Japan). Three images were taken per specimen: one from the central region of the resin–dentin interface, and two others located 300 μm to the left and right.

Quantification of silver deposits within the adhesive and hybrid layers was analyzed by a single calibrated examiner blinded to group assignment. Blinding was achieved by coding all images prior to analysis. Image analysis was performed using ImageJ software (NIH, Bethesda, MD, USA). Original images were converted to 8-bit grayscale, and a consistent thresholding protocol was applied to isolate silver deposits based on pixel intensity.

2.7. In situ degree of conversion (DC)

The resin-dentin bonded sticks were wet-polished, ultrasonically cleaned, and positioned in a micro-Raman microscope (XploRA ONE, HORIBA Scientific; Piscataway, NJ, USA), previously calibrated using a silicon standard. Samples were analyzed using a 532-nm diode laser through a 100x air objective. Raman spectra were acquired using a 600 lines/mm grating over a spectral range of 400- 2000 cm^{-1}. Acquisition settings included 100 mW power, 3 μm spatial resolution, 1 cm^{-1} spectral resolution, and 30-s accumulation with 5 co-additions.

Spectra were collected at three random sites within the hybrid layer of each stick. Post-processing was performed in Opus Spectroscopy Software (version 6.5, HORIBA Scientific; Piscataway, NJ, USA). Spectra from uncured adhesives served as references.

DC was determined from the ratio of aliphatic $C = C$ (1638 cm^{-1}) to aromatic $C = C$ (1608 cm^{-1}) peak intensities in cured and uncured samples ($n = 5$). DC was calculated using the following formula:

$$DC(\%) = (1 - - [R_{cured} / R_{uncured}]) \times 100$$

Where R represent the ratio of aliphatic-to-aromatic peak intensities at 1639 cm^{-1} and 1609 cm^{-1}, respectively [29]. In addition, the more intense peaks and their corresponding chemical bonds were recorded for all materials.

2.8. Statistical analysis

The mean μTBS (MPa), NL (%), and DC (%) values of all bonded sticks from the same tooth quadrant were averaged for statistical analyses, ensuring that each tooth served as the experimental unit. Results corresponding to the two blue-emitting regions (445 and 465 nm) were explored separately; however, all analyses and reporting were ultimately standardized to the actual measured spectral peaks (405, 445, and 465 nm) to avoid ambiguity. The number of specimens experiencing premature failures was low; therefore, we did not include in the calculation. This decision was based on previous evidence [30,31] indicating that when the percentage of premature failures is low (e.g., <10 % of the total specimens), their inclusion does not significantly influence microtensile bond strength outcomes and may otherwise result in biased overestimation. Furthermore, because the tooth was considered the experimental unit and microtensile bond strength values were calculated as the average of all specimens per tooth, the impact of specimen loss due to premature failures was minimized [32]. The μTBS, NL, and DC means for each group were derived from the average of the twenty teeth allocated to each group. For the bonding properties, data were analyzed using a three-way repeated-measures ANOVA (adhesive vs. adhesive strategy vs. wavelength range). The tooth served as the repeated measure because each tooth received all LED wavelengths. Tukey's post hoc test was applied for multiple comparisons, with the level of significance set at $\alpha = 0.05$.

3. Results

3.1. Spectral evaluation

The absolute irradiance (mW/cm^2/nm) and wavelength (nm) emitted by the VALO Cordless unit is shown in Fig. 2. As Fig. 2A illustrates, the device presents three distinct spectral peaks: one near 405 nm, one near 445 nm, and another near 465 nm.

3.2. Microtensile bond strength

Most failures (96 %) were classified as adhesive or mixed (Fig. 3). For the μTBS results, neither the cross-product interaction nor the main factor adhesive strategy was statistically significant (Table 2; $p = 0.61$ and $p = 0.44$, respectively). In contrast, both main factors (i.e. adhesive and wavelength range) were statistically significant (Table 2; $p = 0.001$ and $p = 0.0001$, respectively). Specifically, AMU exhibited higher μTBS values when compared to SBU under both the 405-nm and 445-nm LEDs (Table 2; $p = 0.001$). However, no significant differences were found between 445-nm and 465-nm LEDs for any of the adhesives (Table 2; $p > 0.05$). Conversely, SBU exhibited significantly lower μTBS values when light-cured with the 405-nm LED compared with the 445-nm and 465-nm LEDs (Table 2; $p = 0.001$).

3.3. Nanoleakage values

For NL, neither the cross-product interaction nor the main factors adhesive and adhesive strategy were statistically significant (Table 3; $p = 0.77$, $p = 0.82$, and $p = 0.35$, respectively). However, the main factor wavelength range was statistically significant (Table 3; $p = 0.01$). SBU exhibited significantly higher NL when light-curing with the 405-nm wavelength LED chip compared with other LEDs chips (445 and 465 nm) (Table 3; $p = 0.01$). AMU did not show this wavelength-dependent difference (Table 3; $p > 0.05$).

3.4. In situ degree of conversion

For DC, neither the cross-product interaction nor the main factor adhesive strategy was significant (Table 4; $p = 0.71$ and $p = 0.38$, respectively). In contrast, both main factors, adhesive and wavelength range, were statistically significant (Table 4; $p = 0.001$ and $p = 0.01$, respectively). AMU exhibited higher DC compared to SBU under the 405-nm (in both strategies) and 445-nm LED (etch-and-rinse strategy; Table 4; $p = 0.001$). No significant differences were found among different LEDs for AMU. Conversely, SBU showed significantly lower DC values when light-cured with 405 nm compared with 445 nm and 465 nm (Table 4; $p = 0.01$).

Table 2
Means of microtensile bond strength values (MPa ± standard deviation) for all experimental groups (*).

Wavelength	Ambar Universal APS		Scotchbond Universal	
	Etch-and-rinse	Self-etch	Etch-and-rinse	Self-etch
405 nm	58.5 ± 2.9 a	57.9 ± 2.7 a	40.0 ± 2.8 d	42.7 ± 2.1 d
445 nm	54.7 ± 3.4 ab	54.4 ± 2.3 ab	48.3 ± 3.6 c	48.6 ± 2.3 c
465 nm	54.4 ± 1.2 ab	56.1 ± 2.1 ab	52.9 ± 2.7 bc	52.3 ± 1.2 bc

(*) Different letters indicate statistically different means (three-way ANOVA and Tukey's test; $p < 0.005$).

Table 3
Means of nanoleakage values (% ± standard deviation) for all experimental groups (*).

Wavelength	Ambar Universal APS		Scotchbond Universal	
	Etch-and-rinse	Self-etch	Etch-and-rinse	Self-etch
405 nm	7.3 ± 2.4 a	8.1 ± 2.1 a	14.5 ± 3.2 b	14.7 ± 3.2 b
445 nm	8.2 ± 2.7a	7.3 ± 2.1 a	6.9 ± 1.7 a	9.6 ± 3.5 a
465 nm	8.7 ± 2.4 a	9.2 ± 2.4 a	7.3 ± 2.1 a	6.9 ± 3.2 a

(*) Different letters indicate statistically different means (three-way ANOVA and Tukey's test; $p < 0.005$).

Table 4
Means of degree of conversion values (% ± standard deviation) for all experimental groups (*).

Wavelength	Ambar Universal APS		Scotchbond Universal	
	Etch-and-rinse	Self-etch	Etch-and-rinse	Self-etch
405 nm	68.3 ± 1.4 a	66.3 ± 3.3 a	55.1 ± 3.1 c	56.2 ± 2.9 c
445 nm	65.5 ± 3.5 a	65.6 ± 3.1 a	61.8 ± 3.4 b	63.4 ± 3.7ab
465 nm	66.2 ± 3.7 a	64.3 ± 2.1 a	63.4 ± 3.0 ab	63.4 ± 3.7 ab

(*) Different letters indicate statistically different means (three-way ANOVA and Tukey's test; $p < 0.005$).

4. Discussion

The present study rejected all null hypotheses by demonstrating that

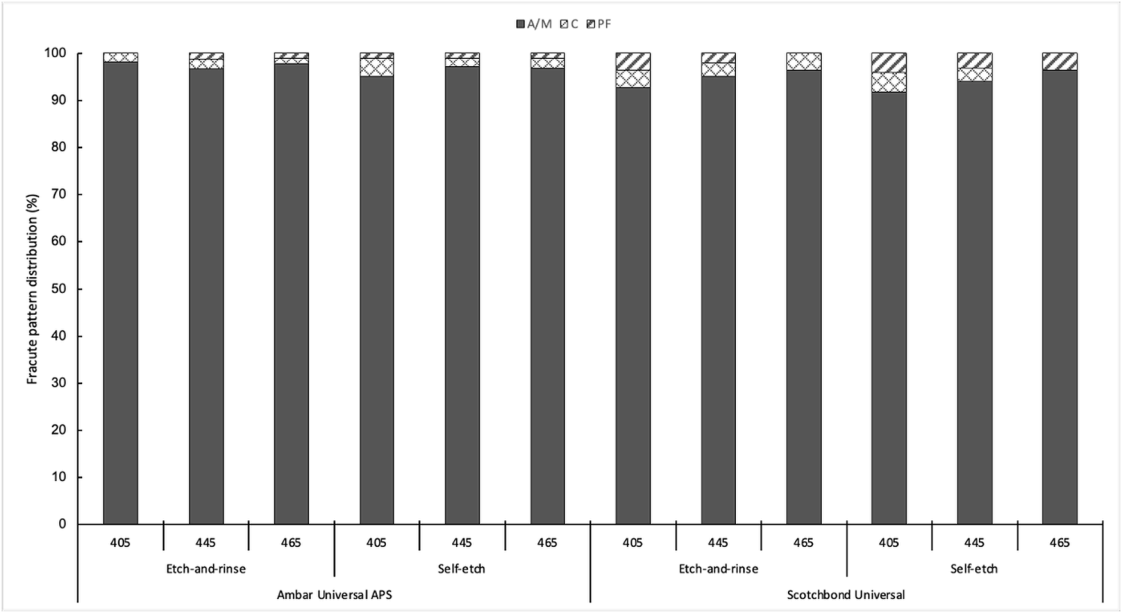

Fig. 3. Fracture pattern distribution (%) for all experimental groups according to the adhesive strategy (Etch-and-rinse, ER or self-etch, SE), and wavelength (405, 445 and 465 nm). A/*M* = Adhesive/mixed failure; *C* = Cohesive failure; PF = premature failure.

localized wavelength ranges emitted by a poly-wave LCU significantly influence the polymerization efficacy and bonding performance of universal adhesives applied to coronal dentin. Light-activated materials must not only receive sufficient radiant energy but must also be exposed to wavelengths that match the absorption spectrum of their PIs to generate an adequate concentration of free radicals for effective polymerization [33]. In the present study, the LCU's tip design prevented a homogeneous distribution of wavelengths across the entire adhesive resin layer covering the dentin substrate [18]. This nonuniform spectral output likely compromised the microtensile bond strength, nanoleakage and degree of conversion behavior of the CQ-containing adhesive.

It is important mention that in the present study, the spectral output of the poly-wave LCU was characterized using a calibrated MARC system at 0 mm to ensure accurate identification of the emitted wavelength ranges. Although the absolute irradiance delivered to each individual tooth quadrant could not be independently isolated due to the integrated beam profile of the device, radiant exposure was standardized across all experimental conditions by maintaining constant curing time, output mode, and tip positioning. Therefore, the observed differences in adhesive performance can be primarily attributed to localized spectral distribution rather than variations in total radiant exposure.

The conversion of monomers into polymers is critical for determining adhesive quality and overall material performance [34], serving as a primary predictor of an adhesive's mechanical integrity and long-term stability [29]. Our findings revealed a significant reduction in the degree of conversion of SBU when light-cured with the 405-nm LED compared with longer wavelengths (i.e. 445 nm and 465 nm). According to the Grotthuss–Draper law (the first law of photochemistry), a photochemical reaction can occur only when the incident light is absorbed by the material [35]. Because violet light (405 nm) lies outside the optimal absorption range of CQ, the incident light insufficiently activates the photoinitiator, resulting in a reduced quantum yield and limited free-radical generation [36]. Consequently, SBU exhibits a lower degree of conversion under violet-light irradiation. Consistent with this mechanism, previous studies have demonstrated that CQ-based PI systems rely predominantly on the blue-light spectral region to achieve maximal polymerization efficiency [37].

In contrast to other tested materials, AMU maintained similar and consistently higher DC values across all three tested wavelengths. This behavior is expected because AMU's formulations present PIs beyond CQ, which reduce its dependence on CQ and broaden the material's spectral responsiveness [37]. Specifically, the Advanced Polymerization System (APS) in AMU combines CQ with phosphine oxide–based initiators that absorb light efficiently in the violet region [34]. These non-CQ PIs exhibit strong molar absorptivity between 350 and 420 nm, a spectral range in which CQ shows markedly reduced absorption. Compared to CQ, the phosphine oxide-based initiators generate far more efficiently, because each absorbed photon yields several initiating species. This higher quantum efficiency accelerates polymerization kinetics, particularly under shorter wavelengths [38,39]. When these initiators operate alongside CQ, it creates an effective synergistic initiation system: the non-CQ initiators dominate radical production under violet illumination, while CQ remains active under blue-light excitation. As a result, radical availability remains high across a wider spectral range, avoiding the wavelength-dependent reduction in polymerization typically observed in CQ-exclusive. Because of this dual-initiator robust mechanism, both violet- and blue-emitting LEDs effectively activate AMU and sustain a high degree of conversion despite differences in emission profile. Such outcome is consistent with numerous studies evaluating this adhesive under comparable conditions [40–42]. This spectral adaptability underscores the superior compatibility and polymerization resilience of multi-initiator adhesive systems when compared to CQ-dependent formulations.

Additionally, a closer examination of the AMU safety data sheet reveals that its formulation includes diphenyl hexafluorophosphate (DPIH), an iodonium-based salt known to act as a co-initiator in light-cured resin systems. Iodonium salts enhance polymerization efficiency because they accelerate PIs decomposition and increase radical generation, ultimately improving the degree of conversion and mechanical properties of adhesive formulations [43,44]. Evidence from studies evaluating the incorporation of diphenyl iodonium salts into experimental adhesives demonstrates substantial improvements in both polymerization kinetics and bond performance, suggesting that such additives can reinforce the adhesive interface under challenging bonding conditions (i.e. uneven wavelength distribution) [45,46]. Thus, the presence of DPIH in AMU indicates a deliberate formulation strategy aimed at enhancing adhesive reactivity and stability, an approach that aligns with the bonding behavior observed in the present investigation and the results observed by Loguercio et al. (2013) [47].

In this context, the degree of conversion directly influences both bond strength and nanoleakage of the universal adhesives evaluated. Factors that promote high bond strength, such as adequate monomer infiltration into demineralized dentin, reduced residual solvent content, and sufficient polymerization, also minimize nanoleakage, as they collectively contribute to a more cohesive and mechanically stable hybrid layer [48,49]. Accordingly, the lower μTBS values observed for SBU at shorter wavelengths are a direct consequence of its deficient polymerization under these conditions [50]. An under-converted polymer network exhibits reduced elastic modulus and flexural strength, limiting its ability to distribute and dissipate interfacial stresses within the hybrid layer, ultimately compromising bond strength [51]. This causal relationship is further supported by the progressive increase in μTBS observed for SBU as the curing wavelength approached its optimal blue-light absorption peak, with markedly higher values at 445 and 460 nm compared to 405 nm.

Furthermore, the nanoleakage results provides additional evidence for this interpretation. When SBU was irradiated with shorter wavelengths, nanoleakage increased, indicating a polymer network layer with low degree of conversion and high permeability. In such networks, unreacted methacrylate groups, incomplete cross-linking, and increased free volume create diffusion pathways that facilitate the movement of water, ions, and other small molecules [52]. Similar findings were reported by Soto-Monteiro et al. [53], who observed significantly elevated nanolakage when a CQ-containing universal adhesive was polymerized with a poly-wave LCU using a regular tip. These defects enhance the deposition of metallic silver grains within the hybrid layer, which is visually expressed as nanoleakage in SEM analyses [28]. In contrast, AMU exhibited consistently low NL values across all wavelengths, reinforcing the superior performance of its multi-initiator photopolymerization systems. By generating a more uniform and densely cross-linked polymer network, it is hypothesized that these systems create an adhesive layer that is both mechanically robust and less permeable, thus preventing fluid infiltration and contributing to a long-term durable and chemically stable hybrid layer [54]. Future studies are needed to validate this hypothesis.

It is worth noting that no significant differences were observed between the etch-and-rinse and self-etch strategies across all experimental groups in most comparisons. This similarity steam from the use of universal adhesives. These adhesives are specifically formulated to perform effectively in both application modes because they contain functional monomers and optimized solvent systems. As a result, they simplify clinical procedures while maintaining comparable bonding effectiveness, allowing clinicians to select the strategy that best suits their preference or clinical requirements [55,56]

From a clinical perspective, the nonuniform spectral output of poly-wave LCUs may be particularly relevant in challenging clinical scenarios, such as deep cavities, subgingival restorations, limited access angles, or situations in which the light tip cannot be positioned perpendicular to the restoration surface [16]. Under these conditions, localized spectral mismatch may impair adhesive polymerization and compromise interfacial integrity, especially in adhesive systems that rely predominantly on CQ-based PI.

In summary, the performance of universal adhesives is critically dependent on the spectral output of the LCU. Poly-wave LCUs, which emit both violet and blue light, are intended to activate a broader range of PIs. But their beam profile often displays inhomogeneously light output distribution. This underscores the need for clinicians to verify the PI composition of the universal adhesive they use, particularly when employing poly-wave lights or when clinical conditions demand deep or uniformly distributed polymerization. However, it is important to note that only one poly-wave LCU was evaluated in this study, which limits the generalizability of the findings. Furthermore, the in vitro design did not incorporate advanced interfacial characterization techniques (e.g., transmission electron microscopy or nanoindentation) and extended aging procedures (e.g., thermocycling or long-term water storage), which are necessary to more comprehensively assess the long-term hydrolytic stability and durability of adhesives interfaces under different spectral conditions.

5. Conclusion

Our findings demonstrate that poly-wave light-curing unit compromises the polymerization efficiency of universal adhesives (SBU) when their heterogeneous wavelength output does not align with the absorption profile of adhesive's photoinitiators. Under this mismatch, camphorquinone-dependent systems displayed a lower degree of conversion, weaker microtensile bond strength, and increased nanoleakage. In contrast, adhesives containing multi-initiator formulations were more tolerant to wavelength variation, maintaining stable bonding performance across all tested wavelengths.

CRediT authorship contribution statement

E Sutil: Writing – original draft, Methodology, Investigation, Conceptualization. **M Wendlinger:** Writing – review & editing, Supervision, Methodology, Conceptualization. **AFM Cardenas:** Writing – original draft, Investigation, Conceptualization. **FSF de Siqueira:** Writing – review & editing, Methodology, Conceptualization. **CJ Soares:** Writing – original draft, Project administration, Conceptualization. **S Geraldeli:** Writing – review & editing, Supervision, Investigation, Conceptualization. **AD Loguercio:** Writing – review & editing, Writing – original draft, Supervision, Project administration, Funding acquisition, Conceptualization.

Declaration of competing interest

The authors declare that they have no known competing financial interests or personal relationships that could have appeared to influence the work reported in this paper.

Acknowledgments

This study was partially supported by the State Foundation of Support to Research, Scientific and Technological Development of Maranhão (FAPEMA) under grant 03628/23 from the State Government of Maranhão Brazil and National Council for Scientific and Technological Development (CNPq) under grant 304444/2025–1 and Coordenação de Aperfeiçoamento de Pessoal de Nível Superior—Brasil (CAPES) – Finance Code 001.

References

[1] W.K. Alomran, M.Z.I. Nizami, H.H.K. Xu, J. Sun, Evolution of dental resin adhesives-a comprehensive review, J. Funct. Biomater. 16 (2025), https://doi.org/10.3390/jfb16030104.
[2] M. Miljkovic, S. Dacic, A. Mitic, D. Petkovic, M. Andjelkovic-Apostolovic, Shear bond strength and failure modes of composite to dentin under different light-curing conditions, Polym. Polym. Compos. 30 (2022) 09673911221143203, https://doi.org/10.1177/09673911221143203.
[3] F.A. Rueggeberg, M. Giannini, C.A.G. Arrais, R.B.T. Price, Light curing in dentistry and clinical implications: a literature review, Braz. Oral Res. 31 (2017) e61, https://doi.org/10.1590/1807-3107BOR-2017.vol31.0061.
[4] E. Fernández Godoy, A. Chaple Gil, R. Caviedes Thomas, C. Bersezio Miranda, J. Martín Casielles, G. Rodríguez Martínez, P. Angel Aguirre, Efficiency and limitations of polywave light-curing units in restorative dentistry: a systematic review, Clin. Oral Investig. 29 (2025) 384, https://doi.org/10.1007/s00784-025-06457-4.
[5] A. Kowalska, J. Sokolowski, K. Bociong, The photoinitiators used in resin based dental composite- a review and future perspectives, Polymers. (Basel) 13 (2021), https://doi.org/10.3390/polym13030470.
[6] K.L. Van Landuyt, J. Snauwaert, J. De Munck, M. Peumans, Y. Yoshida, A. Poitevin, et al., Systematic review of the chemical composition of contemporary dental adhesives, Biomaterials 28 (2007) 3757–3785, https://doi.org/10.1016/j.biomaterials.2007.04.044.
[7] N. Moszner, U. Salz, J. Zimmermann, Chemical aspects of self-etching enamel–dentin adhesives: a systematic review, Dent. Mater. 21 (2005) 895–910, https://doi.org/10.1016/j.dental.2005.05.001.
[8] K.L. Van Landuyt, J. Snauwaert, J. De Munck, E. Coutinho, A. Poitevin, Y. Yoshida, et al., Origin of interfacial droplets with one-step adhesives, J. Dent. Res. 86 (2007) 739–744, https://doi.org/10.1177/154405910708600810.
[9] M.G. Neumann, C.C. Schmitt, G.C. Ferreira, I.C. Corrêa, The initiating radical yields and the efficiency of polymerization for various dental photoinitiators excited by different light curing units, Dent. Mater. 22 (2006) 576–584, https://doi.org/10.1016/j.dental.2005.06.006.
[10] A. Santini, I.T. Gallegos, C.M. Felix, Photoinitiators in dentistry: a review, Prim. Dent. J. 2 (2013) 30–33, https://doi.org/10.1308/205016814809859563.
[11] M. Cadenaro, T. Maravic, A. Comba, A. Mazzoni, L. Fanfoni, T. Hilton, et al., The role of polymerization in adhesive dentistry, Dent. Mater. 35 (2019) e1–e22, https://doi.org/10.1016/j.dental.2018.11.012.
[12] W.F. Schroeder, C.I. Vallo, Effect of different photoinitiator systems on conversion profiles of a model unfilled light-cured resin, Dent. Mater. 23 (2007) 1313–1321, https://doi.org/10.1016/j.dental.2006.11.010.
[13] H. Arikawa, H. Takahashi, T. Kanie, S. Ban, Effect of various visible light photoinitiators on the polymerization and color of light-activated resins, Dent. Mater. J. 28 (2009) 454–460, https://doi.org/10.4012/dmj.28.454.
[14] H.H. Alvim, A.C. Alecio, W.A. Vasconcellos, M. Furlan, J.E. de Oliveira, J.R. Saad, Analysis of camphorquinone in composite resins as a function of shade, Dent. Mater. 23 (2007) 1245–1249, https://doi.org/10.1016/j.dental.2006.11.002.
[15] M.G. Rocha, D. de Oliveira, M. Sinhoreti, J.F. Roulet, A.B. Correr, The combination of CQ-amine and TPO increases the polymerization shrinkage stress and does not improve the depth of cure of bulk-fill composites, Oper. Dent. 44 (2019) 499–509, https://doi.org/10.2341/18-234-l.
[16] R.B. Price, J.L. Ferracane, A.C. Shortall, Light-curing units: a review of what we need to know, J. Dent. Res. 94 (2015) 1179–1186, https://doi.org/10.1177/0022034515594786.
[17] I. Varshney, P. Jha, V. Nikhil, Effect of monowave and polywave light curing on the degree of conversion and microhardness of composites with different photoinitiators: an in vitro study, J. Conserv. Dent. 25 (2022) 661–665, https://doi.org/10.4103/jcd.jcd_223_22.
[18] R.B. Price, D. Labrie, F.A. Rueggeberg, C.M. Felix, Irradiance differences in the violet (405 nm) and blue (460 nm) spectral ranges among dental light-curing units, J. Esthet. Restor. Dent. 22 (2010) 363–377, https://doi.org/10.1111/j.1708-8240.2010.00368.x.
[19] A.C. Shortall, C.J. Felix, D.C. Watts, Robust spectrometer-based methods for characterizing radiant exitance of dental LED light curing units, Dent. Mater. 31 (2015) 339–350, https://doi.org/10.1016/j.dental.2015.02.012.
[20] P.L. Michaud, R.B. Price, D. Labrie, F.A. Rueggeberg, B. Sullivan, Localised irradiance distribution found in dental light curing units, J. Dent. 42 (2014) 129–139, https://doi.org/10.1016/j.jdent.2013.11.014.
[21] R.B. Price, D. Labrie, F.A. Rueggeberg, B. Sullivan, I. Kostylev, J. Fahey, Correlation between the beam profile from a curing light and the microhardness of four resins, Dent. Mater. 30 (2014) 1345–1357, https://doi.org/10.1016/j.dental.2014.10.001.
[22] T. Haenel, B. Hausnerová, J. Steinhaus, R.B. Price, B. Sullivan, B. Moeginger, Effect of the irradiance distribution from light curing units on the local micro-hardness of the surface of dental resins, Dent. Mater. 31 (2015) 93–104, https://doi.org/10.1016/j.dental.2014.11.003.
[23] C.S. Sampaio, P.J. Atria, F.A. Rueggeberg, S. Yamaguchi, M. Giannini, P.G. Coelho, et al., Effect of blue and violet light on polymerization shrinkage vectors of a CQ/TPO-containing composite, Dent. Mater. 33 (2017) 796–804, https://doi.org/10.1016/j.dental.2017.04.010.
[24] P.H.A. Moreira, P.P. Garcia, M.D.N. Correia, N. Chaves, C. Pulido, M.W.C. Ferreira, et al., Long-term evaluation of dentin bonding properties of the photoinitiator system contained in universal adhesives used in Fiber-post luting procedures, J. Adhes. Dent. 25 (2023) 257–266, https://doi.org/10.3290/j.jad.b4786551.
[25] R.F. Carvalho, A. Cardenas, C.N. Carvalho, J.J. de Souza, J. Bauer, F. Siqueira, et al., Effect of the photo-initiator system contained in universal adhesives on radicular dentin bonding, Oper. Dent. 45 (2020) 547–555, https://doi.org/10.2341/19-146-l.
[26] K. Cavalcanti, C. Pulido, P.H.A. Moreira, C.F. Monteles, B.L.C. Salvatierra, F.S. F. Siqueira, et al., Effect of irradiance and exposure time on the adhesive properties of universal adhesives after 2 years of storage, Clin. Oral Investig. 27 (2023) 5223–5232, https://doi.org/10.1007/s00784-023-05142-8.
[27] S. Armstrong, L. Breschi, M. Özcan, F. Pfefferkorn, M. Ferrari, B. Van Meerbeek, Academy of Dental Materials guidance on in vitro testing of dental composite

bonding effectiveness to dentin/enamel using micro-tensile bond strength (μTBS) approach, Dent. Mater. 33 (2017) 133–143, https://doi.org/10.1016/j.dental.2016.11.015.
[28] F.R. Tay, D.H. Pashley, M. Yoshiyama, Two modes of nanoleakage expression in single-step adhesives, J. Dent. Res. 81 (2002) 472–476, https://doi.org/10.1177/154405910208100708.
[29] V. Hass, M. Dobrovolski, C. Zander-Grande, G.C. Martins, L.A. Gordillo, L. Rodrigues Accorinte Mde, et al., Correlation between degree of conversion, resin-dentin bond strength and nanoleakage of simplified etch-and-rinse adhesives, Dent. Mater. 29 (2013) 921–928, https://doi.org/10.1016/j.dental.2013.05.001.
[30] P. Maciel Pires, A. Dávila-Sánchez, V. Faus-Matoses, J.M. Nuñez Martí, L. Lo Muzio, S. Sauro, Bonding performance and ultramorphology of the resin-dentine interface of contemporary universal adhesives, Clin. Oral Investig. 26 (2022) 4391–4405, https://doi.org/10.1007/s00784-022-04402-3.
[31] M. Wendlinger, C. Pomacóndor-Hernández, K. Pintado-Palomino, G.D. Cochinski, A.D. Loguercio, Are universal adhesives in etch-and-rinse mode better than old 2-step etch-and-rinse adhesives? One-year evaluation of bonding properties to dentin, J. Dent. 132 (2023) 104481, https://doi.org/10.1016/j.jdent.2023.104481.
[32] A.D. Loguercio, L.P. Barroso, R.H. Grande, A. Reis, Comparison of intra- and intertooth resin-dentin bond strength variability, J. Adhes. Dent. 7 (2005) 151–158.
[33] R. Nomoto, Effect of light wavelength on polymerization of light-cured resins, Dent. Mater. J. 16 (1997) 60–73, https://doi.org/10.4012/dmj.16.60.
[34] C.M. Tapety, Y.K. Carneiro, Y.M. Chagas, L.C. Souza, N.O. Souza, L.A. Valadas, Degree of conversion and mechanical properties of a commercial composite with an advanced polymerization system, Acta Odontol. Latinoam. 36 (2023) 112–119, https://doi.org/10.54589/aol.36/2/112.
[35] K. LinderstrØM-Lang, Principle of the Cartesian Diver applied to gasometric technique, Nature 140 (1937) 108, https://doi.org/10.1038/140108a0.
[36] Y.-C. Chen, J.L. Ferracane, S.A. Prahl, Quantum yield of conversion of the photoinitiator camphorquinone, Dent. Mater. 23 (2007) 655–664, https://doi.org/10.1016/j.dental.2006.06.005.
[37] V. Miletic, P. Pongprueksa, J. De Munck, N.R. Brooks, B. Van Meerbeek, Monomer-to-polymer conversion and micro-tensile bond strength to dentine of experimental and commercial adhesives containing diphenyl(2,4,6-trimethylbenzoyl)phosphine oxide or a camphorquinone/amine photo-initiator system, J. Dent. 41 (2013) 918–926, https://doi.org/10.1016/j.jdent.2013.07.007.
[38] C.T. Meereis, F.B. Leal, G.S. Lima, R.V. de Carvalho, E. Piva, F.A Ogliari, BAPO as an alternative photoinitiator for the radical polymerization of dental resins, Dent. Mater. 30 (2014) 945–953, https://doi.org/10.1016/j.dental.2014.05.020.
[39] M.A. Hadis, A.C. Shortall, W.M. Palin, The power of light - from dental materials processing to diagnostics and therapeutics, Biomater. Investig. Dent. 11 (2024) 40308, https://doi.org/10.2340/biid.v11.40308.
[40] R.F. Nonato, P.H.A. Moreira, D.O.D. Silva, M.W.C. Ferreira, A. Reis, A.F. M. Cardenas, et al., Long-term evaluation of bonding performance of universal adhesives based on different dentinal moisture levels, J. Adhes. Dent. 24 (2022) 395–406, https://doi.org/10.3290/j.jad.b3559027.
[41] F.S.F. Siqueira, M. Wendlinger, L.C.R. Araújo, P.H.A. Moreira, A.F.M. Cardenas, T. S. Carvalho, et al., Bonding performance of universal adhesives to eroded dentine: a 6-year evaluation, J. Dent. 136 (2023) 104633, https://doi.org/10.1016/j.jdent.2023.104633.
[42] G.C. Cardoso, L. Nakanishi, C.P. Isolan, P.D.S. Jardim, Moraes RR. Bond stability of universal adhesives applied to Dentin using etch-and-rinse or self-etch strategies, Braz. Dent. J. 30 (2019) 467–475, https://doi.org/10.1590/0103-6440201902578.
[43] Q. Ye, J. Park, E. Topp, P. Spencer, Effect of photoinitiators on the in vitro performance of a dentin adhesive exposed to simulated oral environment, Dent. Mater. 25 (2009) 452–458, https://doi.org/10.1016/j.dental.2008.09.011.
[44] D. Kim, A. Scranton, The role of diphenyl iodonium salt (DPI) in three-component photoinitiator systems containing methylene blue (MB) and an electron donor, J. Polym. Sci. Part A: Polym. Chem. 42 (2004) 5863–5871.
[45] F.A. Ogliari, C. Ely, G.S. Lima, M.C. Conde, C.L. Petzhold, F.F. Demarco, E. Piva, Onium salt reduces the inhibitory polymerization effect from an organic solvent in a model dental adhesive resin, J. Biomed. Mater. Res. B Appl. Biomater. 86 (2008) 113–118, https://doi.org/10.1002/jbm.b.30995.
[46] F.A. Ogliari, C. Ely, C.L. Petzhold, F.F. Demarco, E. Piva, Onium salt improves the polymerization kinetics in an experimental dental adhesive resin, J. Dent. 35 (2007) 583–587, https://doi.org/10.1016/j.jdent.2007.04.001.
[47] A.D. Loguercio, R. Stanislawczuk, F.G. Mittelstadt, M.M. Meier, A. Reis, Effects of diphenyliodonium salt addition on the adhesive and mechanical properties of an experimental adhesive, J. Dent. 41 (2013) 653–658, https://doi.org/10.1016/j.jdent.2013.04.009.
[48] G. Cochinski, M. Wendlinger, E. Kaizer, T. Carneiro, P. Moreira, A. Cardenas, et al., Does the absence of HEMA in universal adhesive systems containing MDP affect the bonding properties to enamel and dentine? A one-year evaluation, Int. J. Adhes. Adhes. 132 (2024) 103656.
[49] M. Wendlinger, A. Nuñez, P. Moreira, T.S. Carneiro, G.D. Cochinski, F. Siqueira, et al., Effect of the absence of HEMA on the bonding properties of universal adhesive systems containing 10-MDP: an In vitro study, Oper. Dent. 48 (2023) 500–512, https://doi.org/10.2341/22-050-l.
[50] Faleiros DdM, C.C. Schmitt, M.G. Neumann, Influence of the photoinitiator concentration on the mechanical and optical properties of dental resins, Mater. Res. 24 (2021) e20210188.
[51] M. Moldovan, R. Balazsi, A. Soanca, A. Roman, C. Sarosi, D. Prodan, et al., Evaluation of the degree of conversion, residual monomers and mechanical properties of some light-cured dental resin composites, Materials. (Basel) 12 (2019), https://doi.org/10.3390/ma12132109.
[52] M. Cadenaro, F. Antoniolli, S. Sauro, F.R. Tay, R. Di Lenarda, C. Prati, et al., Degree of conversion and permeability of dental adhesives, Eur. J. Oral Sci. 113 (2005) 525–530, https://doi.org/10.1111/j.1600-0722.2005.00251.x.
[53] J. Soto-Montero, G. Nima, C.T.S. Dias, R.B.T. Price, M. Giannini, Influence of beam homogenization on bond strength of adhesives to dentin, Dent. Mater. 37 (2021) e47–e58, https://doi.org/10.1016/j.dental.2020.10.003.
[54] S. Sauro, S. Vijay, S. Deb, Development and assessment of experimental dental polymers with enhanced polymerisation, crosslink density and resistance to fluid permeability based on ethoxylated-bisphenol-A-dimethacrylates and 2-hydroxyethyl methacrylate, Eur. Polym. J. 48 (2012) 1466–1474, https://doi.org/10.1016/j.eurpolymj.2012.05.013.
[55] A. Wagner, M. Wendler, A. Petschelt, R. Belli, U. Lohbauer, Bonding performance of universal adhesives in different etching modes, J. Dent. 42 (2014) 800–807, https://doi.org/10.1016/j.jdent.2014.04.012.
[56] L. Breschi, T. Maravic, C. Mazzitelli, U. Josic, E. Mancuso, M. Cadenaro, et al., The evolution of adhesive dentistry: from etch-and-rinse to universal bonding systems, Dent. Mater. 41 (2025) 141–158, https://doi.org/10.1016/j.dental.2024.11.011.